

Surface plasmon polaritons induced reduced hacking

Bakhtawar, Muhammad Haneef, and Humayun Khan

Citation: Chin. Phys. B, 2021, 30 (**6**): 064215. DOI: 10.1088/1674-1056/abd7e5
Journal homepage: http://cpb.iphy.ac.cn; http://iopscience.iop.org/cpb

What follows is a list of articles you may be interested in

Broadband asymmetric transmission for linearly and circularly polarization based on sand-clock structured metamaterial

Tao Fu(傅涛), Xing-Xing Liu(刘兴兴), Guo-Hua Wen(文国华), Tang-You Sun(孙堂友), Gong-Li Xiao(肖功利), and Hai-Ou Li(李海鸥)

Chin. Phys. B, 2021, 30 (**1**): 014201. DOI: 10.1088/1674-1056/abb662

Ultra wide sensing range plasmonic refractive index sensor based on nano-array with rhombus particles

Jiankai Zhu(朱剑凯), Xiangxian Wang(王向贤), Xiaoxiong Wu(吴枭雄), Yingwen Su(苏盈文), Yueqi Xu(徐月奇), Yunping Qi(祁云平), Liping Zhang(张丽萍), and Hua Yang(杨华)$

Chin. Phys. B, 2020, 29 (**11**): 114204. DOI: 10.1088/1674-1056/abb229

A theoretical study of a plasmonic sensor comprising a gold nano-disk array on gold film with a SiO_2 spacer

Xiangxian Wang(王向贤), Jiankai Zhu(朱剑凯), Huan Tong(童欢), Xudong Yang(杨旭东), Xiaoxiong Wu(吴枭雄), Zhiyuan Pang(庞志远), Hua Yang(杨华), Yunping Qi(祁云平)

Chin. Phys. B, 2019, 28 (**4**): 044201. DOI: 10.1088/1674-1056/28/4/044201

Geometrical condition for observing Talbot effect in plasmonics infinite metallic groove arrays

Afshari-Bavil Mehdi, Xiao-Ping Lou(娄小平), Ming-Li Dong(董明利), Chuan-Bo Li(李传波), Shuai Feng(冯帅), Parsa Saviz, Lian-Qing Zhu(祝连庆)

Chin. Phys. B, 2018, 27 (**12**): 124204. DOI: 10.1088/1674-1056/27/12/124204

Tunable graphene-based mid-infrared band-pass planar filter and its application

Somayyeh Asgari, Hossein Rajabloo, Nosrat Granpayeh, Homayoon Oraizi

Chin. Phys. B, 2018, 27 (**8**): 084212. DOI: 10.1088/1674-1056/27/8/084212

Surface plasmon polaritons induced reduced hacking

Bakhtawar, Muhammad Haneef†, and Humayun Khan

Lab of Theoretical Physics, Hazara University Mansehra, 21300 KP, Pakistan

(Received 2 September 2020; revised manuscript received 24 December 2020; accepted manuscript online 4 January 2021)

There is always need for secure transmission of information and simultaneously compact-size photonic circuits. This can be achieved if surface plasmon-polaritons (SPPs) are used as source of information, and the reduced hacking as the transmission phenomenon. In this article, an SPP-based reduced hacking scheme is presented at interface between atomic medium and metallic conductor. The SPP propagation is manipulated with conductivity of the metal. The delay or advance of the SPP is found to create nanosecond time gap which can be used for storing and sending the information safely. The reduced hacking is further modified with conductivity of the metal and the control parameters of the atomic medium.

Keywords: surface plasmons, coherent control of atomic interactions with photons, reduced hacking, surface conductivity

PACS: 42.50.–p, 71.36.+c **DOI:** 10.1088/1674-1056/abd7e5

1. Introduction

Are these modes capable of secure transmission of information, the reduced hacking? This is a well known phenomenon in which information can be hacked from external detectors through a trick of light.[1,2] The idea of reduced hacking was first introduced by McCall *et al*. using the concept of light splitting into slow and fast components.[3] This was experimentally demonstrated using optical fibers based on dispersion[4] as well as polarization control of a probe beam.[5] After the experimental demonstration of reduced hacking, several research groups put their efforts for the realization of photonic devices capable of achieving hacking.[6–8] It simultaneously attracted tremendous theoretical interest for its proper description and modification. For example, Li *et al*.[9] reported a reduced hacking scheme based on quantum destructive interference in a three-level warm atomic system where a reduced hacking was created in a long optical pulse propagating in the system. Wu and Wang demonstrated their reduced hacking scheme using the Fourier analysis method.[10] Chremmos presented a scheme where biconvex temporal gaps were created continuously in a medium having positive or negative dispersion.[11] In a previous work, our colleagues have discussed creation of the reduced hacking between the enhanced subluminal and superluminal pulse caused by the Doppler broadening in atomic medium.[12]

However, a question whether it is possible to construct a reduced hacking device that can work for surface plasmon polaritons (SPPs) arises. SPPs are electromagnetic modes that arise due to the interaction between light and collective oscillations of free electrons in a metal. They are bound to the surface of the conductor and prevent power to propagate away from the surface.[13,14] SPPs have generated remarkable interest for their ability to manipulate light at subwavelength scales, leading to nanophotonic devices with length scales much smaller than those achievable with ordinary light.[15,16]

So for, SPPs have found numerus applications in polarizers, sensors, photodetectors, spectroscopy, microscopy, metasurfaces, compact cameras, integrated imaging, and detection systems.[17–34] With these remarkable properties, SPPs can present some exciting opportunities for efficient reduced hacking. With this in mind, in this article we present a theoretical approach towards the reduced hacking based on SPPs. We consider the interface between a coherently driven four-level atomic medium and a metallic conductor where propagation of the SPPs is manipulated with conductivity of the metal and the control parameters of the atomic medium. The advantage of using a coherent treatment is that one has different controlling parameters in hand to manipulate the plasmonic modes.[35–37] We show that event cloaking is possible for the surface modes at the interface between the two media. Our results show improvement/development towards the plasmonstor based reduced hacking technology which may be of interest for the researchers working in either of the two fields, reduced hacking and surface science.

This paper is organized as follows. In Section 2, we define the geometry and present analytical expressions for describing both media above and below the interface. It is followed by the dispersion relation of surface plasmon together with the description for the reduced hacking. In Section 3, we present and discuss the results of the study. In Section 5, we summarize the results.

2. Model and analytical expressions

The schematic diagram of Fig. 1(a) shows the interface between a metallic conductor and an atomic medium along

†Corresponding author. E-mail: haneef.theoretician@gmail.com

© 2021 Chinese Physical Society and IOP Publishing Ltd

which SPPs are excited. The conducting medium is characterized by complex conductivity σ, complex electric permittivity $\varepsilon_{\rm m}$ and magnetic permeability $\mu_{\rm m}$. It is supposed that it obeys the source free Maxwell equations. When a probe field is incident on the coupled surface, it causes variations in the complex conductivity σ and permittivity $\varepsilon_{\rm m}$ of the metal. The wave equations for the electric and magnetic field components inside the conducting medium can be written as

$$\nabla^2 E = \mu_{\rm m}\varepsilon_{\rm m}\frac{\partial^2 E}{\partial t^2} + \mu_{\rm m}\sigma\frac{\partial E}{\partial t}, \tag{1}$$

$$\nabla^2 B = \mu_{\rm m}\varepsilon_{\rm m}\frac{(\partial^2 B)}{\partial t^2} + \mu_{\rm m}\sigma\frac{\partial B}{\partial t}. \tag{2}$$

The solutions to Eqs. (1) and (2) are the model with plane wave time dependence $E_{\rm m}(r,t) = E_{0\rm m}\,{\rm e}^{{\rm i}k_{\rm m}r-\omega t}$ and $B_{\rm m}(r,t) = B_{0\rm m}\,{\rm e}^{{\rm i}k_{\rm m}r-\omega t}$, where $E_{0\rm m}$ and $B_{0\rm m}$ stand for complex amplitudes for the electric and magnetic fields inside the metal. Further, $k_{\rm m}$ represents the complex wave vector of the probe field and can be written as[36]

$$k_{\rm m}^2 = \mu_{\rm m}\varepsilon_{\rm m}\omega^2 + {\rm i}\mu_{\rm m}\sigma\omega, \tag{3}$$

where ω is the angular frequency of the probe field. To include the phase dependence, the complex permittivity and permeability of the metal are written as $\varepsilon_{\rm m} = \varepsilon_0\varepsilon_{\rm rm}$ and $\mu_{\rm m} = \mu_0\mu_{\rm rm}$; ε_0 and μ_0 are the permittivity and permeability of the free space. The terms $\varepsilon_{\rm rm}$ and $\mu_{\rm rm}$ represent complex dielectric and permeability constants. In polar form $\varepsilon_{\rm rm} = |\varepsilon_{\rm rm}|\,{\rm e}^{\beta_1}$, $\mu_{\rm rm} = |\mu_{\rm rm}|\,{\rm e}^{\beta_2}$, $\sigma = |\sigma|\,{\rm e}^{\beta_3}$. Here $|\varepsilon_{\rm rm}|$ and $|\sigma|$ represent amplitudes of complex dielectric and permeability constants, $|\mu_{\rm rm}|$ is the amplitude of complex conductivity, and $\beta_{1,2,3}$ are corresponding phase of these quantities. Plugging these values in Eq. (3) we obtain

$$k_{\rm m}^2 = \mu_0\omega(G_1 + {\rm i}G_2). \tag{4}$$

Since $k_{\rm m}$ is also a complex quantity and can be expressed as $k_{\rm m} = k_{1\rm m} + {\rm i}k_{2\rm m}$, the expressions for its real and imaginary parts are calculated by

$$k_{1\rm m} = \pm\sqrt{\frac{\mu_0\omega(G_1 \pm \sqrt{G_1^2+G_2^2})}{2}}, \tag{5}$$

$$k_{2\rm m} = \pm\sqrt{\frac{\mu_0\omega(-G_1 \pm \sqrt{G_1^2+G_2^2})}{2}}. \tag{6}$$

In Eqs. (4)–(6), the constant terms are defined as

$$\begin{aligned} G_1 &= \varepsilon_0\omega|\mu_{\rm rm}||\varepsilon_{\rm rm}|\cos(\beta_1+\beta_2) \\ &\quad -|\mu_{\rm rm}||\sigma|\sin(\beta_2+\beta_3), \end{aligned} \tag{7}$$

$$\begin{aligned} G_2 &= \varepsilon_0\omega|\mu_{\rm rm}||\varepsilon_{\rm rm}|\sin(\beta_1+\beta_2) \\ &\quad +|\mu_{\rm rm}||\sigma|\cos(\beta_2+\beta_3). \end{aligned} \tag{8}$$

If $n_{\rm r}^m$ is the refractive index of the conducting medium, then $k_{\rm m} = k_0 n_{\rm r}^m$, where $k_0 = \omega/c = 2\pi/\lambda$ is the free space wave number of the incident light. Using the above relations the refractive index of the conducting medium is calculated by

$$\begin{aligned} n_{\rm r}^m &= \pm\sqrt{\frac{\mu_0 c^2(G_1 \pm \sqrt{G_1^2+G_2^2})}{2\omega}} \\ &\quad \pm{\rm i}\sqrt{\frac{\mu_0 c^2(-G_1 \pm \sqrt{G_1^2+G_2^2})}{2\omega}}. \end{aligned} \tag{9}$$

Further we assume a four-level atomic whose energy level diagram as shown in Fig. 1(b). It can be experimentally realized in four energy levels in the D lines of ^{87}Rb atom.[38,39] The same configuration was used recently for the manipulation of SPP's solitary waves[40] as well as for subluminal and superluminal SPP propagation.[36] Here, a probe field $E_{\rm p}$ having Rabi frequency $\Omega_{\rm p}$ is coupled with states $|2\rangle$ and $|3\rangle$. A control field E_1 having Rabi frequency Ω_1 is applied between the states $|1\rangle$ and $|3\rangle$ while the control field E_2 of Rabi frequency Ω_2 couples the states $|2\rangle$ and $|4\rangle$. The spontaneous decay rates between the coresponding states are denoted by γ_{31}, γ_{32}, γ_{41} and γ_{42} as shown in the figure.

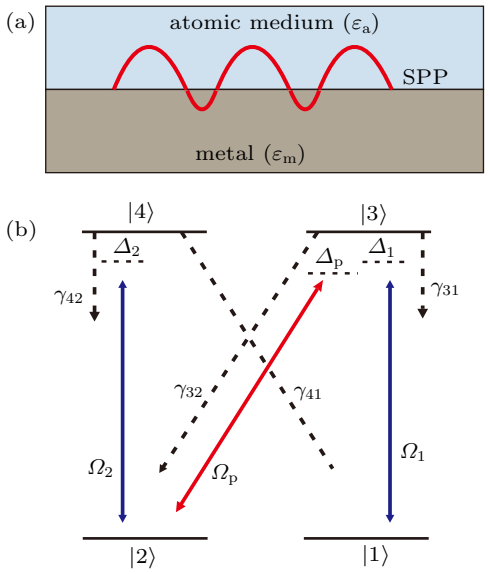


Fig. 1. (a) The interface between a metal and the atomic medium where SPPs are generated. (b) Energy diagram of four-level atomic system.

The self energy part of Hamiltonian of this atomic configuration is

$$H_0 = \sum_{m=1}^{4}\hbar\omega_m|m\rangle\langle m|, \tag{10}$$

whereas its Hamiltonian in the interaction picture is

$$\begin{aligned} H_I &= -\frac{\hbar}{2}[\Omega_1\,{\rm e}^{-{\rm i}\Delta_1 t}|1\rangle\langle 3| + \Omega_{\rm p}\,{\rm e}^{-{\rm i}\Delta_{\rm p}t}|2\rangle\langle 3| \\ &\quad +\Omega_2\,{\rm e}^{-{\rm i}\Delta_2 t}|2\rangle\langle 4| + {\rm H.c.}]. \end{aligned} \tag{11}$$

Here, $\Omega_{\rm p} = d_{23}E_{\rm p}/\hbar$, $\Omega_1 = d_{31}E_1/\hbar$ and $\Omega_2 = d_{24}E_2/\hbar$; d_{23}, d_{31}, and d_{24} are the dipoles matrix elements between the states

$|\mathrm{i}\rangle$ and $|j\rangle$. $\Delta_{1,2,p}$ represent the detuning frequencies of the corresponding fields.

The master density matrix equation used for the dynamical solution of the system is given by[41]

$$\dot{\rho} = -\frac{\mathrm{i}}{\hbar}[H_i,\rho] - \sum \frac{1}{2}\gamma_{ij}(Q^{\dagger}Q\rho + \rho Q^{\dagger}Q - 2Q\rho Q^{\dagger}), \quad (12)$$

where $Q^{\dagger}$ (Q) is the raising (lowering) operator. After straight forward algebraic manipulation, the coupling equations for the given system can be obtained as follows:[40]

$$\dot{\widetilde{\rho}}_{23} = \kappa_1\widetilde{\rho}_{23} - \frac{\mathrm{i}}{2}\Omega_2\widetilde{\rho}_{43} + \frac{\mathrm{i}}{2}\Omega_1\widetilde{\rho}_{21} + \frac{\mathrm{i}}{2}\Omega_{\mathrm{p}}(\widetilde{\rho}_{22} - \widetilde{\rho}_{33}), \quad (13)$$

$$\dot{\widetilde{\rho}}_{21} = \kappa_2\widetilde{\rho}_{21} + \frac{\mathrm{i}}{2}\Omega_1^*\widetilde{\rho}_{23} - \frac{\mathrm{i}}{2}\Omega_2\widetilde{\rho}_{41} - \frac{\mathrm{i}}{2}\Omega_{\mathrm{p}}\widetilde{\rho}_{31}, \quad (14)$$

$$\dot{\widetilde{\rho}}_{43} = \kappa_3\widetilde{\rho}_{43} + \frac{\mathrm{i}}{2}\Omega_1\widetilde{\rho}_{41} + \frac{\mathrm{i}}{2}\Omega_{\mathrm{p}}\widetilde{\rho}_{42} + \frac{\mathrm{i}}{2}\Omega_2^*\widetilde{\rho}_{23}, \quad (15)$$

$$\dot{\widetilde{\rho}}_{41} = \kappa_4\widetilde{\rho}_{41} + \frac{\mathrm{i}}{2}\Omega_1^*\widetilde{\rho}_{43} - \frac{\mathrm{i}}{2}\Omega_2^*\widetilde{\rho}_{21}. \quad (16)$$

The dot on each element represents its time derivative and Ω_i^* stands for complex conjugate of Ω_i. Here, we assume that the atoms are initially prepared in state $|2\rangle$ for a weak probe electric field, i.e., $\Omega_{\mathrm{p}} << \gamma_{ij}$. Under this condition, only $\widetilde{\rho}_{22}^{(0)} = 1$ while the terms $\widetilde{\rho}_{33,31,42}^{(0)}$ all go to zero due to small Rabi oscillations. Solving relations (13)–(16), the probe field coherence is calculated as

$$\widetilde{\rho}_{23}^{(1)} = \frac{2\mathrm{i}[4\kappa_2\kappa_3\kappa_4 + \kappa_2\Omega_1^2 + \kappa_3\Omega_2^2]\Omega_{\mathrm{p}}}{\kappa_5\Omega_1^2 + \Omega_1^4 + (4\kappa_1\kappa_3 - \Omega_2^2)(4\kappa_2\kappa_4 + \Omega_2^2)}. \quad (17)$$

Using relation (17), the complex electric susceptibility of the system can be expressed as

$$\chi = \frac{2Nd_{23}^2\widetilde{\rho}_{23}^{(1)}}{\varepsilon_0\hbar\Omega_{\mathrm{p}}}, \quad (18)$$

where N stands for the density of atoms in the atomic ensemble and d_{23}^2 is dipole matrix element. The dispersion relation for the SPPs is given by

$$k_{\mathrm{sp}} = \frac{2\pi}{\lambda}\sqrt{\frac{\varepsilon_{\mathrm{a}}(n_{\mathrm{r}}^m)^2}{\varepsilon_{\mathrm{a}} + (n_{\mathrm{r}}^m)^2}}, \quad (19)$$

where $\varepsilon_{\mathrm{a}} = 1 + \chi$. From Eq. (19), the refractive index of the SPP can be written as $n_{\mathrm{r}}^{(\mathrm{sp})} = k_{\mathrm{sp}}/k_0$ and its phase velocity as $v_{\mathrm{sp}} = c/n_{\mathrm{r}}^{(\mathrm{sp})}$. Furthermore, the SPP group index can be obtained as

$$n_{\mathrm{g}}^{(\mathrm{sp})} = \mathrm{Re}[n_{\mathrm{r}}^{(\mathrm{sp})}] + \omega_0\,\mathrm{Re}\left[\frac{\partial n_{\mathrm{r}}^{(\mathrm{sp})}}{\partial\omega}\right], \quad (20)$$

where ω_0 is the central frequency of the probe field. Next, a propagating SP at the interface can be expressed as

$$S_{\mathrm{i}}(t) = \frac{1}{\sqrt{2\pi}}\int_{-\infty}^{\infty} S_{\mathrm{i}}(\Delta_{\mathrm{p}})\,\mathrm{e}^{-\mathrm{i}\Delta_{\mathrm{p}}t}\,\mathrm{d}\Delta_{\mathrm{p}}, \quad (21)$$

where $S_{\mathrm{i}}(t)$ is taken Gaussian pulse have width τ_0 in time domain while

$$S_{\mathrm{i}}(\Delta_{\mathrm{p}}) = \int_{-\infty}^{\infty} S_{\mathrm{i}}(t)\,\mathrm{e}^{\mathrm{i}\Delta_{\mathrm{p}}t}\,\mathrm{d}t \quad (22)$$

in frequency domain.

Delay or advancement of the SP is caused by the phase shift in frequency domain. Therefore, if $S(t)$ is the propagating SP, a phase shift $\mathrm{e}^{\pm\mathrm{i}\omega\Delta t^{(\mathrm{sp})}}$ is created due to the fact that delay or advancement of the SP is caused nearly at the central time t_0. To create a time window in the SP transmission spectrum, the transfer function at the interface of two media can be obtained as

$$T(\Delta_{\mathrm{p}}) = \begin{cases} \exp[-\mathrm{i}\Delta_{\mathrm{p}}(\Delta t^{(\mathrm{sp})}], & t > t_0, \\ \exp[\mathrm{i}\Delta_{\mathrm{p}}(\Delta t^{(\mathrm{sp})}], & t < t_0. \end{cases} \quad (23)$$

The transmission spectrum $S_{\mathrm{tr}}(\Delta_{\mathrm{p}})$ of the pulse $S_{\mathrm{i}}(\Delta_{\mathrm{p}})$ is written as

$$S_{\mathrm{tr}}(\Delta_{\mathrm{p}}) = S_{\mathrm{i}}(\Delta_{\mathrm{p}})T(\Delta_{\mathrm{p}}), \quad (24)$$

which can be further written in time domain via the Fourier transform

$$S_{\mathrm{tr}}(t) = F^{-1}[S_{\mathrm{i}}(\Delta_{\mathrm{p}})T(\Delta_{\mathrm{p}})]. \quad (25)$$

This is a piece-wise continuous function and therefore, phase shift theorem is applied to $S_{\mathrm{tr}}(t)$ which results in the subsequent ranges[42]

$$S_{\mathrm{tr}}(t) = \begin{cases} S_{\mathrm{i}}(t - \Delta t^{(\mathrm{sp})}), & t > t_0 + \Delta t^{(\mathrm{sp})}, \\ 0, & t_0 - \Delta t^{(\mathrm{sp})} < t < t_0 + \Delta t^{(\mathrm{sp})}, \\ S_{\mathrm{i}}(t + \Delta t^{(\mathrm{sp})}), & t < t_0 - \Delta t^{(\mathrm{sp})}. \end{cases}$$

This relation shows that the transmission frequency spectrum is zero in the time interval $t_0 - \Delta t^{(\mathrm{sp})} < t < t_0 + \Delta t^{(\mathrm{sp})}$. This interval is the created time gap which is double of the pulse delay or advance time, i.e., $2\Delta t^{(\mathrm{sp})}$, where the information can be transmitted without any detection. If any event $S_{\mathrm{e}}(t)$ is transmitted within this gap, then the expression becomes $S_{\mathrm{e}}(t)S_{\mathrm{tr}}(t) = 0$, which shows that the event $S_{\mathrm{e}}(t)$ has no effect on the transmission frequency spectrum and can be safely transmitted without hacking. To close the time gap another interface is required whose transfer function is complex conjugation of the original transfer function. This will reverse the process and remove the time gap.

3. Results and discussion

In this section we present and discuss the results obtained on the basis of the analytical expressions of the previous section. The parameters $\kappa_1 = \mathrm{i}\Delta_{\mathrm{p}} - (\gamma_{32} + \gamma_{42})/2$, $\kappa_2 = \mathrm{i}(\Delta_1 - \Delta_{\mathrm{p}}) + (\gamma_{32} + \gamma_{31} + \gamma_{42} + \gamma_{41})/2$, $\kappa_3 = \mathrm{i}(\Delta_2 - \Delta_{\mathrm{p}})$, $\kappa_4 = \mathrm{i}(\Delta_1 + \Delta_2 - \Delta_{\mathrm{p}}) + (\gamma_{31} + \gamma_{41})/2$ and $\kappa_5 = 4(\kappa_1\kappa_2 + \kappa_3\kappa_4)$. Propagation of the surface waves, their absorbtion, dispersion,

group index and delay/advance time are investigated at the interface of the proposed media. Time gap in the delay or advancement of the SPP is also manipulated. For numerical results, we adopt a spontaneous decay rate of $\gamma = 1$ MHz and scale other parameter of the atomic medium with this γ. Other common parameters assumed for the study are $\Delta_{1,2} = 0\gamma$, $\Omega_1 = 3.5\gamma$, $\Omega_2 = 0.5\gamma$ and $\mu_{\rm rm} = 1$. Moreover, the decay terms are taken to be $\gamma_{ij} = 2\gamma$.[38] The phases of the complex quantities related to the conducting medium are kept as $\beta_1 = 0$, $\beta_2 = \pi/3$ and $\beta_3 = \pi/4$. The conductivity of the metal is expressed in units of S/m.

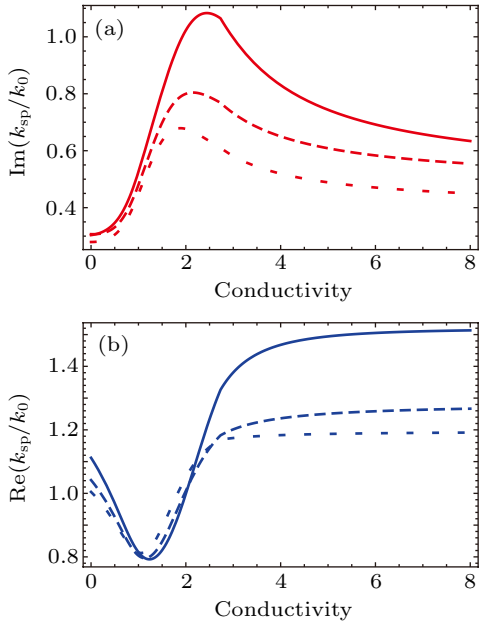


Fig. 2. Absorption and dispersion behavior of surface plasmon polariton versus conductivity of the metal such that $\Delta_p = 0\gamma$ (solid line), $\Delta_p = 0.5\gamma$ (dashed line) and $\Delta_p = 0.8\gamma$ (dotted line).

The probe field, coupling the states $|2\rangle$ and $|3\rangle$ of the atomic medium, decays evanescently along the interface and excites SPs. Absorption and dispersion behaviors of the surface modes are plotted against conductivity of the conducting medium as shown in Fig. 2. The imaginary Im(k_{sp}) shows absorption and real part Re(k_{sp}) shows dispersion spectrum of the SPP. A single maximum of the absorption and minimum of the dispersion spectra are noticed near $\sigma = 2$ S/m at specific parameters of the proposed media. However, the peaks in the dispersion curves can be shifted to higher values of the metal's conductivity as seen from dashed and dotted curves. With increasing the conductivity further, the dispersion spectrum finally becomes saturated and the surface mode acquires a fixed character.

Figure 3 shows group index and delay/advance time of the SPP. The plots show that group index and delay/advance time is positive at low values of the metal conductivity and negative at higher values and become saturated at increasing the conductivity further, which is in agreement with the previous results. At resonance $\Delta_p = 0\gamma$ in the atomic medium, the group index is -637.5 at conductivity of the metal $\sigma = 3.96$ S/m and is noted to be -272 and -80 at the probe detuning frequencies $\Delta_p = 0.5\gamma$ and $\Delta_p = 0.8\gamma$, respectively, for the same value of conductivity. This shows that the plasmon delays and advances during its propagation along the interface. The value of advance time at the interface at resonance is -20×10^{-8} s while at $\Delta_p = 0.5\gamma$ the same value of conductivity is 10×10^{-8} s. At $\Delta_p = 0.8\gamma$ delay time of 5×10^{-8} s is noted. Furthermore, the mode propagation is noted to change between the superluminal and subluminal propagation by varying the probe detuning in the atomic medium at the specific value of conductivity in the metallic medium.

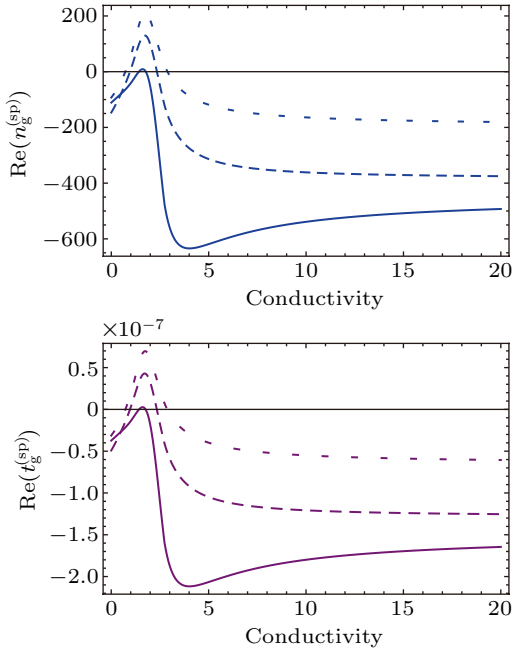


Fig. 3. Group index and group delay/advance time of surface plasmon polariton versus conductivity of the metal. Other parameters are kept the same as in Fig. 2.

In Fig. 4, we plot the normalized intensities of the generated plasmonic pulse, its transmission at the interface and the final output pulse versus time. The time t is normalized by the probe field width τ_0, which is assumed to be 25 ns in this case. The upper plot (red curve) shows the initially excited plasmonic pulse in time domain. The transmission is denoted by the three curves blue, green and purple, in the central portion of this figure, for different values of probe field detunings. Note that a temporal window can be created for the plasmonic pulse which splits for an arbitrary time during its transmission. The front part of the pulse speeds up while its back part slows down, the so-called superluminal and subluminal propagation. Time gaps of 400 ns, 200 ns and 100 ns are generated at the advance/delay times of 20×10^{-8} s, 10×10^{-8} s and 5×10^{-8} s for probe field detuning $\Delta_p = 0\gamma$, $\Delta_p = 0.5\gamma$ and $\Delta_p = 0.8\gamma$, respectively. This shows that the time gaps can be conveniently controlled by adjusting different parameter related to the atomic medium. These time gaps provide the

necessary durations for an event to occur and can be made hidden from external detectors. The initial form of the pulse can be restored by reversing the whole process. In other words, when the time gape is closed the original information can be restored as shown in the final plot, showing output SPP pulse intensity.

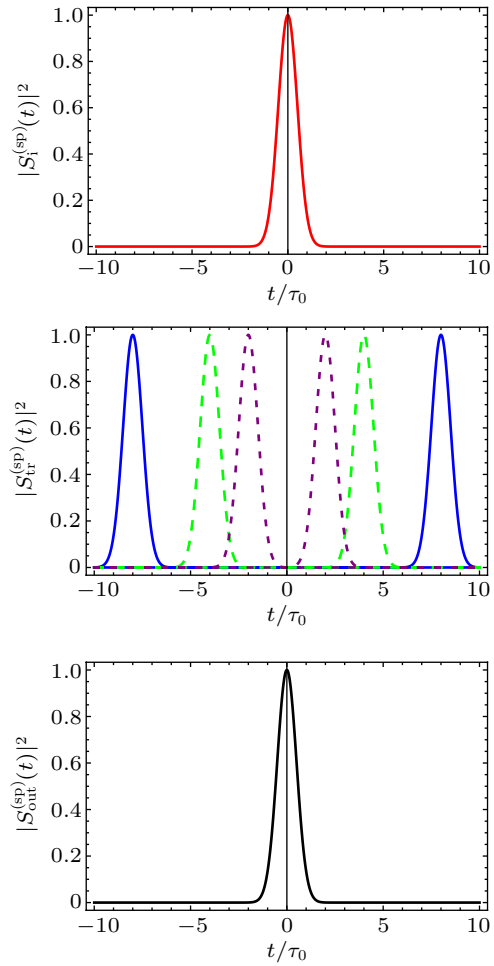


Fig. 4. The normalized SPP pulse, its transmission and output intensities versus t/τ_0 such that $\tau_0 = 25$ ns, $\Delta_{\rm p} = 0\gamma$ (blue solid line), $\Delta_{\rm p} = 0.5\gamma$ (green dashe line) and $\Delta_{\rm p} = 0.8\gamma$ (purple dotted line).

In Fig. 5 we show how the normalized intensities of the generated SPP pulse, its transmission through the interface and the output pulse intensities can be manipulated with different probe field widths. Here, the probe field is assumed to be resonantly coupled and conductivity of the metal is kept constant at $\sigma = 3.96$ S/m. We find that the time gap decreases as the probe width is increased, and vice versa, as shown in the central part of Fig. 5. The transmission pulse intensity remains zero for long duration of time when the pulse width is kept small and hence a comparatively larger time gap is created. The time gap is closed by the reverse process and the initial SPP pulse is obtained in its original form as shown in the lower plot. This shows that the time gap for the event cloaking can be well manipulated with varying width of the probe field. Moreover, as the properties of the SPPs are shown to depend on conductivity of the metal (Fig. 2), the cloaking phenomenon can also be controlled by conductivity of the metal.

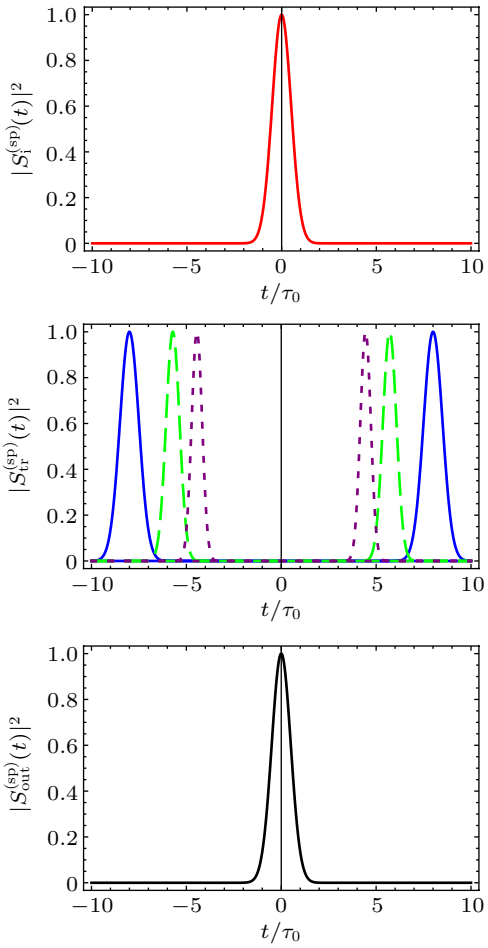


Fig. 5. The normalized SPP pulse, its transmission and output intensities versus t/τ_0 such as $\Delta_{\rm p} = 0\gamma$, $\tau_0 = 25$ ns (blue solid line), $\tau_0 = 35$ ns (green dashed line), and $\tau_0 = 45$ ns (purple dotted line).

4. Conclusions

In summary we have investigated reduced hacking based on SPPs propagating along the interface between a four-level atomic medium and a metallic conductor. We have modified the SPPs propagation with conductivity of the metal. Further, a plasmonic pulse is noticed to delay and advance in time during its propagation at the interface. This delay and advance of the pulse lead to the creation of the time gap for reduced hacking. Temporal gaps of the orders of nanoseconds are measured for reduced hacking of plasmonic waves. These gaps are noted to be further modified with conductivity of the metal, detuning frequency and width of the probe field. The time gaps are also closed by the reverse process. Our results may have potential applications in nanoscale-sized devices for storing or sending secure information. Comparisons with the previous methods and published articles are present. In this work, we have modified the reducing hacking by surface Plasmon polariton at the interface of atomic and metallic media. In the methods of other works the frequencies are used to modify the

cloaking. Here the metal conductivity along with frequencies plays an important role for the modification reducing hacking. Further we have used here piece wise continuous function for SPPs at the interface. A nano second time gap is control for SPPs, which is very large as compared to its decay.

References

[1] McCall M 2013 *Contemp. Phys.* **54** 273
[2] Merali Z 2013 *Nature*
[3] McCall M W, Favaro A, Kinsler P and Boardman A 2010 *J. Opt.* **13** 024003
[4] Fridman M, Farsi A, Okawachi Y and Gaeta A 2012 *Nature* **481** 62
[5] Bony P Y, Guasoni M, Morin P, Sugny D, Picozzi A, R Jauslin H, Pitois S and Fatome J 2014 *Nat. Commun.* **5** 4678
[6] Boyd R and Shi Z 2012 *Nature* **481** 35
[7] Lukens J M, Leaird D and M Weiner A 2013 *Nature* **498** 205
[8] Lukens J M, Metcalf A J, Leaird D E and Weiner A M 2014 *Optica* **1** 372
[9] Li R B, Deng L, Hagley E W, Bienfang J C, Payne M G and Ge M L 2013 *Phys. Rev. A* **87** 023839
[10] Wu K and Wang G P 2013 *Opt. Express* **21** 238
[11] Chremmos I 2014 *Opt. Lett.* **39** 4611
[12] Jabar M S A, Bacha B A and Ahmad I 2015 *Laser Physics* **25** 065405
[13] Maier S A 2007 *Plasmonics: Fundamentals and Applications* (Berlin: Springer)
[14] Jabar M S A and Bacha B A 2018 *J. Opt.* **20** 12
[15] Barnes W L, Dereux A and Ebbesen T W 2003 *Nature* **424** 824
[16] Tame M S, McEnery K, Ozdemir S, Lee J, Maier S and Kim M 2013 *Nat. Phys.* **9** 329
[17] Liedberg B, Nylander C and Lunstrom I 1983 *Sensors & Actuat.* **4** 299
[18] Cai W, Genov D A and Shalaev V M 2005 *Phys. Rev. B* **72** 193101
[19] Kurokawa Y and Miyazaki H T 2007 *Phys. Rev. B* **75** 035411
[20] Zeng X, Al-Amri M and Zubairy M S 2014 *Phys. Rev. B* **90** 235418
[21] Zeng X, Fan L and Zubairy M S 2017 *Phys. Rev. A* **95** 053850
[22] Bakhtawar, Haneef M, Bacha B A, Khan H and Atif M 2018 *Chin. Phys. B* **27** 114215
[23] Yao Y, Shen Y, Hao J M and Dai N 2019 *Acta Phys. Sin.* **68** 147802 (in Chinese)
[24] Zhang W J, Gao L, Wei H and Xu H X 2019 *Acta Phys. Sin.* **68** 147302 (in Chinese)
[25] Li P 2019 *Acta Phys. Sin.* **68** 146201 (in Chinese)
[26] Guo Y, Zhang Z, Pu M, Huang Y, Li X, Ma X and Xu M Luo X 2019 *Iscience* **21** 145
[27] He P H, Zhang H C, Gao X X, *et al.* 2019 *Opto-electron Adv.* **2** 190001
[28] Luo X G 2015 *Sci. Chin.-Phys., Mech. Astron.* **58** 594201
[29] Khan H, Haneef M and Bakhtawar 2018 *Chin. Opt. Lett.* **17** 032701
[30] Shoaib B, Haneef M, Bacha B A, Khan H and Bakhtawar 2019 *Commun. Theor. Phys.* **71** 435
[31] Khan R, Iqbal M, Haneef M, Bacha B A, Khan H, Bakhtawar and Mariam 2019 *Laser Phys.* **29** 045403
[32] Khan H, Haneef M and Bakhtawar 2018 *Chin. Phys. B* **27** 014201
[33] Khan H and Haneef M 2017 *Laser Phys.* **27** 055201
[34] Khan H, Haneef M and Bakhtawar 2019 *Chin. Opt. Lett.* **17** 032701
[35] Din R U, Zeng X D, Ge G Q and Zubairy M S 2019 *Opt. Express* **27** 322
[36] Khan N, Bacha B A, Iqbal A, Rahman A U and Afaq A 2017 *Phys. Rev. A* **96** 013848
[37] Din R U, Badshah F, Ahmad I and Ge G Q 2018 *Europhys. Lett.* **122** 17001
[38] Agarwal G S and Dasgupta S 2004 *Phys. Rev. A* **70** 023802
[39] Sheng J, Yang X, Khadka U and Xiao M 2011 *Opt. Express* **19** 17059
[40] Ahmad S, Ahmad A, Bacha B A, Khan A A, Abdul M and Jabar S 2017 *Eur. Phys. J. Plus* **132** 506
[41] Scully M and Zubairy M S 1997 *Quantum Optics* (Cambridge: Cambridge University Press)
[42] Gustafson S C 1996 *Opt. Eng.* **35** 1513